Cyclopentadienyl Oxides of Molybdenum

Frank Bottomley,* Edith C. Ferris, and Peter S. White

Department of Chemistry, University of New Brunswick, Fredericton, New Brunswick, Canada E3B 5A3

Received September 19, 1989

An improved preparation of $CpMoCl_2(O)$ (Cp = η-C_5H_5) from $[MoCl_3(O)]_n$ and $Bu^n{}_3Sn(C_5H_5)$ is described. X-ray diffraction revealed that $CpMoCl_2(O)$ has a piano-stool structure similar to $Cp^*VCl_2(O)$ and $Cp^*ReCl_2(O)$ (Cp^* = η-$C_5(CH_3)_5$). The major difference between the three compounds is the Cl–M–Cl angle, 104.6 (2)° in $Cp^*VCl_2(O)$ (d^0), 93.4 (1)° in $CpMoCl_2(O)$ (d^1), and 85.4 (1)° in $Cp^*ReCl_2(O)$ (d^2). Extended Hückel molecular orbital calculations showed that the decrease in the Cl–M–Cl angle as the number of d electrons increased is due to occupation of an orbital that is π-antibonding between M and Cl at high Cl–M–Cl angles but weakly σ-bonding at low angles. Reduction of $CpMoCl_2(O)$ with zinc powder in tetrahydrofuran (THF) gave diamagnetic $\{[CpMoCl]_4(\mu\text{-}O)_6\}(ZnCl(THF))_2$, formally containing two Mo(IV) and two Mo(V) centers. Reoxidation of $\{[CpMoCl]_4(\mu\text{-}O)_6\}(ZnCl(THF))_2$ with O_2 gave green $[CpMoCl(O)]_2(\mu\text{-}O)$ (containing two Mo(V) centers), colorless $[ZnCl(THF)(\mu\text{-}Cl)]_\infty$, and a third black product that could not be identified. X-ray diffraction showed that $[CpMoCl(O)]_2(\mu\text{-}O)$ was centrosymmetric with a linear Mo–O–Mo bridge and was diamagnetic. The relation between the center of symmetry and the diamagnetism is discussed.

Introduction

We have been investigating the preparation and properties of organometallic oxides.[1,2] A key compound of this type is the antiferromagnetic cluster $[CpCr(\mu_3\text{-}O)]_4$ (Cp = η-C_5H_5).[3-5] To understand the properties of this cluster it is desirable to prepare the molybdenum analogue. However, all preparations of $[CpCr(\mu_3\text{-}O)]_4$ involve oxidation of Cp_2Cr, whose molybdenum analogue is not known. An alternative approach to $[CpMo(\mu_3\text{-}O)]_4$ appeared to be reductive aggregation of the known $CpMoCl_2(O)$,[6-8] a procedure that has been successfully used to prepare $[CpTi]_6(\mu_3\text{-}O)_8$ from $[CpTiCl_2]_2(\mu\text{-}O)$.[9] We report here on a convenient preparation of $CpMoCl_2(O)$, a comparison of its structure with the related $Cp^*VCl_2(O)$[10] and $Cp^*ReCl_2(O)$[11] (Cp^* = η-$C_5(CH_3)_5$), the reduction of $CpMoCl_2(O)$ with zinc (in the presence of zinc oxide) to give $\{[CpMoCl]_4(\mu\text{-}O)_6\}(ZnCl(THF))_2$, and the reoxidation of the latter to $[CpMo(O)Cl]_2(\mu\text{-}O)$ and $[ZnCl(THF)(\mu\text{-}Cl)]_\infty$.

Results and Discussion

Preparation and Structure of $CpMoCl_2(O)$. Green and co-workers have reported several methods of preparation of $CpMoCl_2(O)$.[6-8] However the highest yield reported was 15%. Modification of the procedure reported by Bunker and Green,[7] in which $CpMoCl_2(O)$ was obtained but not isolated from $[MoCl_3(O)]_n$ and $Bu^n{}_3Sn(C_5H_5)$ (eq 1) gave yields of 40% on a regular basis, with occasional

$$[MoCl_3(O)]_n + n(Bu^n)_3Sn(C_5H_5) \rightarrow n[(\eta\text{-}C_5H_5)MoCl_2(O)] + n(Bu^n)_3SnCl \quad (1)$$

preparations yielding 50%. Though still not ideal, the synthesis is a one-pot preparation from commercially available $[MoCl_3(O)]_n$ and the readily prepared $Bu^n{}_3Sn(C_5H_5)$.[12] The complex $CpMoCl_2(O)$ is best identified by ν(Mo=O) at 946 cm^{-1}; other useful spectroscopic properties are a broad proton NMR signal at 48 ppm and a broad single-line ESR signal at g = 1.96.

Table I. Distances (Å) and Angles (deg) in $CpMoCl_2(O)$

Mo–O	1.740 (6)	Cl(1)–Mo–Cl(2)	93.4 (1)
Mo–Cl(1)	2.306 (3)	O–Mo–Cl(1)	103.4 (3)
Mo–Cl(2)	2.297 (3)	O–Mo–Cl(2)	102.8 (3)
Mo–Cp	2.054	O–Mo–Cp	122.7
		Cl(1)–Mo–Cp	114.3
		Cl(2)–Mo–Cp	115.6

Table II. Distances (Å) and Angles (deg) in $Cp'MCl_2(O)$ Compounds

	$Cp^*VCl_2(O)$[a]	$CpMoCl_2(O)$[b]	$Cp^*ReCl_2(O)$[c]
Cl–M–O	103.4 (4)	103.1 (3)	105.7 (2)
Cl–M–Cl	104.6 (2)	93.4 (1)	85.4 (1)
Cl–M–Cp[d]	112.6	114.9	111.1
O–M–Cp[d]	118.7	122.7	128.9
M–O	1.576 (8)	1.740 (6)	1.700 (4)
M–Cl	2.224 (5)	2.302 (2)	2.346
M–Cp	2.009	2.054	1.972

[a] Reference 10. [b] This work. [c] Reference 11. [d] The strong trans effect of the oxygen ligand means that neither the M–C nor the C–C distances are equal. There is also disorder in the Cp ring of $CpMoCl_2(O)$. The values for M–Cp, O–M–Cp, and Cl–M–Cp were calculated by using the centroid of the C_5 ring, obtained from the coordinates of the five ring carbon atoms. Since internal consistency rather than absolute value is important, this method appears most suitable.

It was found that $CpMoCl_2(O)$ crystallized in a variety of unit cells, all of which were disordered to a greater or lesser degree. The disorder is best described by noting that $CpMoCl_2(O)$ is a piano stool in which one leg (the oxygen atom) is much shorter than the other two (see Figure 1 and Table I). When such stools are stacked, there is a tendency for them to slip when rotation of the legs does not keep the seats parallel. In the crystals of $CpMoCl_2(O)$ this slippage resulted in 90–95% occupancy of a particular site by a $CpMoCl_2(O)$ molecule, with the remaining 5–10% of the molecules occupying one or more positions translated by approximately 1 Å from the major site. The data reported in the Experimental Section and the distances and

---

[1] Bottomley, F.; Paez, D. E.; White, P. S. *J. Am. Chem. Soc.* **1985**, *107*, 7226.

[2] Bottomley, F.; Drummond, D. F.; Paez, D. E.; White, P. S. *J. Chem. Soc., Chem. Commun.* **1986**, 1752.

[3] Fischer, E. O.; Ulm, F.; Fritz, H. P. *Chem. Ber.* **1960**, *93*, 2167.

[4] Bottomley, F.; Paez, D. E.; White, P. S., *J. Am. Chem. Soc.* **1981**, *103*, 5581.

[5] Bottomley, F.; Paez, D. E.; White, P. S. *J. Am. Chem. Soc.* **1982**, *104*, 5651.

[6] Cousins, M.; Green, M. L. H. *J. Chem. Soc.* **1964**, 1567.

[7] Bunker, M. J.; Green, M. L. H., *J. Chem. Soc., Dalton Trans.* **1981**, 847.

[8] Green, M. L. H.; Knight, J.; Segal, J. A. *J. Chem. Soc., Dalton Trans.* **1977**, 2189.

[9] Roth, A.; Floriani, C.; Chiesi-Villa, A.; Guastini, C. *J. Am. Chem. Soc.* **1986**, *108*, 6823.

[10] Bottomley, F.; Darkwa, J.; Sutin, L.; White, P. S. *Organometallics* **1986**, *5*, 2165.

[11] Herrmann, W. A.; Küsthardt, U.; Flöel, M.; Kulpe, J.; Herdtweck, E.; Voss, E. *J. Organomet. Chem.* **1986**, *314*, 151.

[12] Fritz, H. P.; Kreiter, C. G. *J. Organomet. Chem.* **1964**, *1*, 323.

0276-7333/90/2309-1166$02.50/0

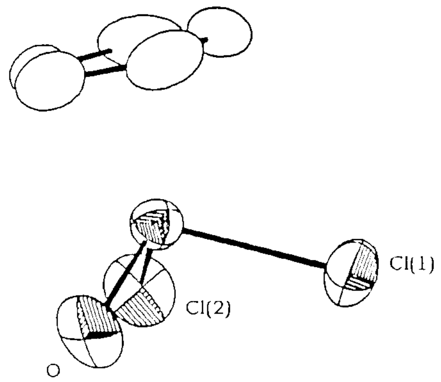

Figure 1. Molecular structure of $CpMoCl_2(O)$.

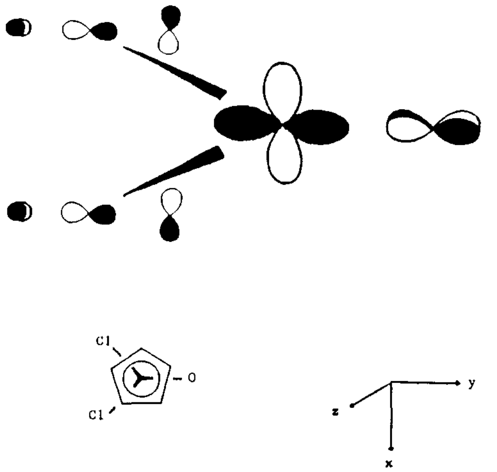

Figure 2. Contributions of chlorine and metal orbitals to the LUMO of $CpNbCl_2(O)$.

angles given in Table I were from a crystal showing the minimum of disorder and only over one subsidiary site.

Although the disorder in the crystals of $CpMoCl_2(O)$ precludes a detailed discussion of the intramolecular parameters, a number of clear and interesting conclusions emerge from a comparison between the structures of $CpMoCl_2(O)$, $Cp^*VCl_2(O)$,[10] and $Cp^*ReCl_2(O)$.[11] Table II gives the data. It is seen that the Cl–M–O and Cl–M–Cp angles vary very little in the three compounds (the maximum range is 3.8°). The O–M–Cp angle varies 10°, from 119° in $Cp^*VCl_2(O)$ (d^0) through 123° in $CpMoCl_2(O)$ (d^1), to 129° in $Cp^*ReCl_2(O)$ (d^2). The largest variation is in the Cl–M–Cl angle, which is 105° in $Cp^*VCl_2(O)$, 93° in $CpMoCl_2(O)$, and 85° in $Cp^*ReCl_2(O)$. It is difficult to interpret the changes in the metal–ligand distances because of the very different radii of the metals. However, with covalent radii from the same source (V 1.25; Mo 1.45; Re 1.59; O 0.73; Cl 0.99 Å[13]) it appears that the M–O distances are approximately equal. The V–Cl distance is that expected for a single bond; the Mo–Cl and Re–Cl distances are, however, considerably longer (0.14 and 0.23 Å, respectively) than expected.

Table III. Total Electronic Energy and Energy (eV) of the LUMO of $CpNbCl_2(O)$ as a Function of the Cl–Nb–Cl Angle (deg)

angle	energy of LUMO (A)	total energy (B)	$A + B$	$2A + B$
75	−10.973 77	−918.770 80	−929.744 57	−940.718 34
80	−10.847 12	−919.337 69	−930.184 81	−941.031 93
85	−10.729 72	−919.679 69	−930.409 41	−941.139 13
90	−10.623 40	−919.880 73	−930.504 13	−941.127 53
95	−10.529 35	−919.989 35	−930.518 70	−941.048 05
100	−10.449 09	−920.033 59	−930.482 68	−940.931 77
103.4	−10.403 62	−920.035 16	−930.438 78	−940.842 40
105	−10.385 67	−920.029 08	−930.414 75	−940.800 42
110	−10.344 03	−919.983 77	−930.327 80	−940.671 83
115	−10.328 58	−919.900 20	−930.228 78	−940.557 36

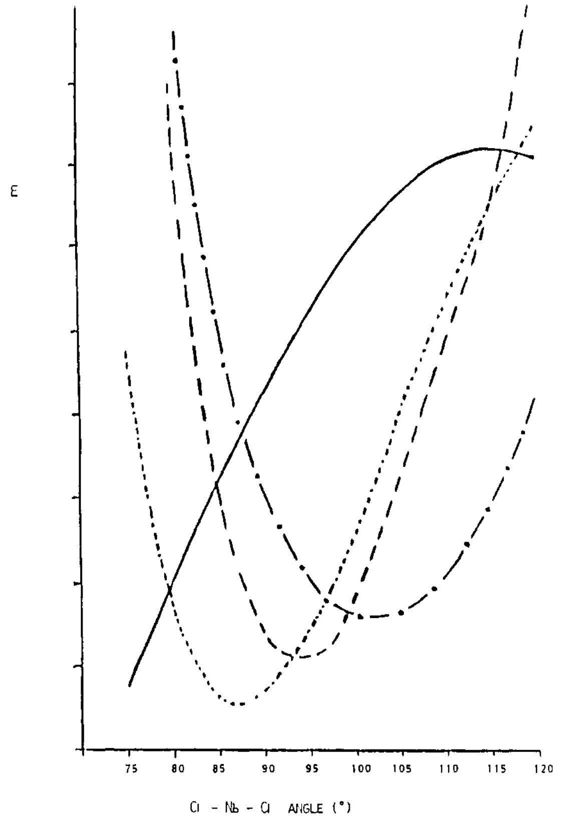

Figure 3. Variation in the total energy (–·–), energy of the LUMO (—), total + LUMO energy (– – –), and total + 2(LUMO) energy (···) for $CpNbCl_2(O)$.

We turn first to the most marked variation, the Cl–M–Cl angle. This has been examined by using extended Hückel molecular orbital methods. To avoid any steric problems, $CpNbCl_2(O)$ was used as the model d^0 compound, with the axis scheme shown in Figure 2. The ordering of the (empty) d orbital energy levels for $CpNbCl_2(O)$ is $d_{x^2-y^2}$ (−10.404 eV) < d_{xy} (−10.143) < d_{z^2} (−10.031) ≪ d_{xz} (−7.584) ~ d_{yz} (−7.121). This ordering follows from the involvement of d_{xz} and d_{yz} in the bonding to Cp and the σ bonds to Cl and O and the involvement of d_{xy} and d_{z^2} in π-bonding to O. The LUMO of $CpNbCl_2(O)$ is the $d_{x^2-y^2}$ orbital, this being occupied by one electron in $CpMoCl_2(O)$ and two in $Cp^*ReCl_2(O)$. The variations in the total electronic energy and in the energy of the LUMO of $CpNbCl_2(O)$ are given in Table III and plotted as a function of the Cl–Nb–Cl angle in Figure 3. Combining these energies gives the curves for the d^1 and d^2 cases also shown in Figure 3. It is seen that the total energy (the d^0 case) has a minimum at a Cl–M–Cl angle of approximately 102°, the sum of the total energy and the LUMO energy (the d^1 case) at 93° and the sum of the total energy and twice the LUMO energy (the d^2 case) at 87°, in very satisfying agreement with the experimental values of 105, 93, and 85°, respectively. The minimum energy shifts with the number of d electrons because the energy of LUMO of $CpNbCl_2(O)$ increases markedly as the Cl–Nb–Cl angle increases. The reason for this increase can be seen from the contributions of the various atomic orbitals to the LUMO, which are given in Table IV. The major contribution is from $d_{x^2-y^2}$, but as

---

(13) Butler, I. S.; Harrod, J. F. *Inorganic Chemistry*; Benjamin/Cummings: Redwood, CA, 1989; p 48.

Table IV. Contribution of the Atomic Orbitals (%) to the LUMO of $CpNbCl_2(O)$ as a Function of the Cl–Nb–Cl Angle (deg)

	Nb			Cl		
angle	$x^2 - y^2$	z^2	yz	z	y	x
75	60	23	2	4	5	8
80	60	22	3	5	6	8
85	60	20	4	6	7	7
90	60	18	5	6	9	7
95	61	14	6	6	11	6
100	63	10	7	6	13	5
103.4	65	6	9	5	14	4
105	66	4	9	5	15	4
110	68	0	11	3	16	3
115	66	2	11	0	16	2

the Cl–Nb–Cl angle increases, the contribution from d_{z^2} decreases from 20% to zero, whereas the contribution from d_{yz} rises (from 3 to 10%), as does the contribution of the Cl p_y orbital (from 6 to 16%). Varying the Cl–Nb–Cl angle has little effect on any interaction between Cl orbitals and d_{z^2}, but as is clear from Figure 2, the interaction between the Cl p_y orbitals and $d_{x^2-y^2}$ and between Cl p_y and d_{yz} changes from weakly bonding to antibonding as the Cl–Nb–Cl angle increases. Thus the LUMO of $CpNbCl_2(O)$ will be pushed to higher energy with increased Cl–Nb–Cl angle.

The relatively long Re–Cl and Mo–Cl distances, compared to V–Cl, are probably only a reflection of the smaller Cl–M–Cl angles; intramolecular nonbonding repulsion between the Cl ligands forces them to move away from the metal center. Such nonbonding (i.e., steric) repulsion is however only a second-order effect. If it was the determining factor, we would expect the largest X–M–X angle for the largest X and the smallest metal. However the I–Re–I angle in $Cp^*ReI_2(O)$ is 88.8 (1)°,[14] only 3.4° larger than in $Cp^*ReCl_2(O)$,[11] and the Cl–Mo–Cl angle of 93.4° is greater than the Cl–Re–Cl angle in $Cp^*ReCl_2(O)$, although Mo is larger than Re.

We analyzed the Cp–M–O angle in a manner similar to the Cl–M–Cl angle. However the variation in both the total energy and the energy of the LUMO with the Cp–Nb–O angle was so small that no reasonable minimum could be found. The EHMO calculations suggest that the Cp–M–O angle is not an important factor in the bonding of these $CpMX_2(O)$ molecules. Neither have we been able to find any relationship between the Cl–M–Cl or Cp–M–O angles and the M–O distance.

Reduction of $CpMoCl_2(O)$. On reduction with zinc powder in tetrahydrofuran (THF), $CpMoCl_2(O)$ slowly gave red-brown $\{[CpMoCl]_4(\mu\text{-}O)_6\}(ZnCl(THF))_2$. The unusual formulation for the product is supported by several lines of evidence. Microanalyses (C, H, Cl) agreeing with this formulation were consistent and reproducible, and the negative-ion FAB mass spectrum strongly supported it. Oxidation of $\{[CpMoCl]_4(\mu\text{-}O)_6\}(ZnCl(THF))_2$ by O_2 *in toluene* gave green $[CpMoCl(O)]_2(\mu\text{-}O)$ (Figure 4) and colorless $[ZnCl(THF)(\mu\text{-}Cl)]_\infty$, which were conclusively identified by X-ray crystallography, and a third black product, which could not be conclusively identified. The structure of $[CpMoCl(O)]_2(\mu\text{-}O)$ is discussed below; that of $[ZnCl(THF)(\mu\text{-}Cl)]_\infty$ was reported elsewhere.[15] The oxidation in toluene was reproducible; therefore the $ZnCl_2(THF)$ unit must be present in the product of the reduction of $CpMoCl_2(O)$ by zinc powder. The NMR spectra of the reduction product also showed the presence of coordinated THF, though when the product was recrystallized from THF/ether, coordinated ether was also evident. This indicated that the THF was labile, which probably accounts for the somewhat low molecular weight (1080, calculated 1228) determined osmometrically. Note that $Cp_4Mo_4Cl_6O_6Zn_2$ (i.e., without THF) has a molecular weight of 1084. $\{[CpMoCl]_4(\mu\text{-}O)_6\}(ZnCl(THF))_2$ was diamagnetic. This provides further evidence for the tetranuclear nature of the product, which contains formally a mixture of Mo(IV) and Mo(V) and has a total of six cluster electrons. In contrast to $CpMoCl_2(O)$, the reduction product showed no ν(Mo═O) vibrations in the infrared spectrum, only Mo–O–Mo bridging vibrations at 728 cm^{-1}. There were no ν(O–H) vibrations. Two structures for $\{[CpMoCl]_4(\mu\text{-}O)_6\}(ZnCl(THF))_2$ can be proposed. One is an adamantane-like configuration for the $[CpMoCl]_4(\mu\text{-}O)_6$ units, with the Zn^{2+} bridging opposite edges of the tetrahedron of CpMoCl groups. Adamantane-like structures have been observed in $[Cp^*M]_4(\mu_2\text{-}O)_6$ (M = Ti,[16] V[17]). The other possible structure is the rectangular configuration shown in Figure 5. The proton NMR spectrum showed two resonances of equal intensity at 6.44 and 6.38 ppm in the C_5H_5 region. We conclude that the two resonances arise from conformationally different $\eta\text{-}C_5H_5$ rings in $\{[CpMoCl]_4(\mu\text{-}O)_6\}(ZnCl(THF))_2$. Such conformationally different rings are not possible with a highly symmetrical adamantane structure but are readily allowed by the rec-

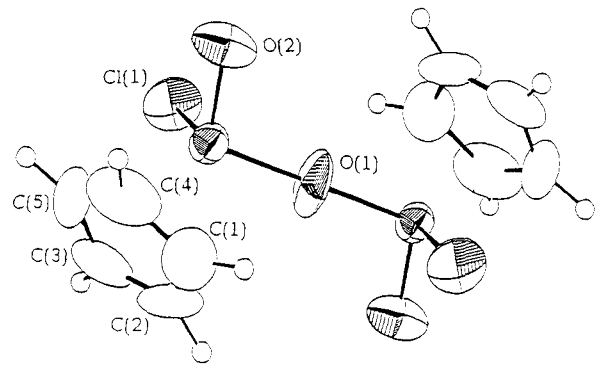

Figure 4. Molecular structure of $[CpMoCl(O)]_2(\mu\text{-}O)$.

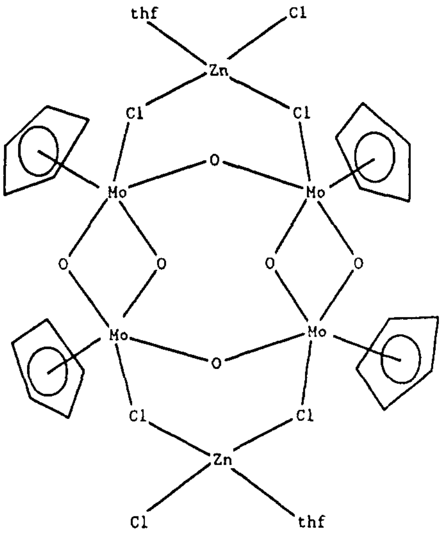

Figure 5. Proposed structure of $\{[CpMoCl]_4(\mu\text{-}O)_6\}(ZnCl(THF))_2$.

---

[14] Herrmann, W. A.; Herdtweck, E.; Flöel, M.; Kulpe, J.; Küsthardt, U.; Okuda, J. *Polyhedron* **1987**, *6*, 1165.

[15] Bottomley, F.; Ferris, E. C.; White, P. S. *Acta Crystallogr.* **1989**, *45C*, 816.

[16] Babcock, L. M.; Day, V. W.; Klemperer, W. G. *J. Chem. Soc., Chem. Commun.* **1987**, 858.

[17] Bottomley, F.; Magill, C. P.; Zhao, B. Submitted for publication in *Organometallics*.

Table V. Important Distances (Å) and Angles (deg) in $[\mathrm{CpMoCl(O)}]_2(\mu\text{-O})$

Mo–O(1)	1.847 (1)	O(1)–Mo–O(1A)	180.0
Mo–O(2)	1.668 (7)	O(1)–Mo–O(2)	108.1 (3)
Mo–Cl	2.348 (3)	O(1)–Mo–Cl	90.4 (1)
Mo–C(1)	2.328 (12)	O(2)–Mo–Cl	105.5 (3)
Mo–C(2)	2.410 (10)		
Mo–C(3)	2.411 (12)		
Mo–C(4)	2.319 (11)		
Mo–C(5)	2.329 (12)		

tangular structure of Figure 5. For instance, chair, boat, or planar forms are possible, and the $\mathrm{Zn^{2+}}$ may bridge either the edges having single or those having double oxygen bridges. In all cases except a completely planar $\mathrm{Mo_4Zn_2}$ framework the $\mathrm{C_5H_5}$ rings will be conformationally different, depending on whether they are above or below the $\mathrm{Mo_4}$ frame.

$\{[\mathrm{CpMoCl}]_4(\mu\text{-O})_6\}(\mathrm{ZnCl(THF)})_2$ contains two Mo(V) and two Mo(IV) centers but has more oxygen per molybdenum than does the Mo(V) complex $\mathrm{CpMoCl_2(O)}$. Thus a redistribution reaction appears to have taken place on reduction of $\mathrm{CpMoCl_2(O)}$ with zinc powder. However, this would require the breaking of Mo–O bonds, which seems unlikely. A more plausible source of oxygen is from the zinc powder used in the reduction. This inevitably has a surface coating of ZnO that cannot be removed. The reduction would then be described by eq 2.

$$4\mathrm{CpMoCl_2(O)} + \mathrm{Zn} + 2\mathrm{ZnO} + 2\mathrm{THF} \rightarrow \{[\mathrm{CpMoCl}]_4(\mu\text{-O})_6\}(\mathrm{ZnCl(THF)})_2 + \mathrm{ZnCl_2} \tag{2}$$

Oxidation of $\{[\mathrm{CpMoCl}]_4(\mu\text{-O})_6\}(\mathrm{ZnCl(THF)})_2$ with $\mathrm{O_2}$ reproducibly gave green $[\mathrm{CpMoCl(O)}]_2(\mu\text{-O})$, colorless $[\mathrm{ZnCl(THF)}(\mu\text{-Cl})]_\infty$, and a black amorphous, paramagnetic solid. The first two products were conclusively identified. To preserve the stoichiometry of the reaction, a third compound, $[\mathrm{CpMo(O)_2}]_2$, must be produced (eq 3). The

$$2\{[\mathrm{CpMoCl}]_4(\mu\text{-O})_6\}(\mathrm{ZnCl(THF)})_2 + \mathrm{O_2} \rightarrow 2[\mathrm{CpMoCl(O)}]_2(\mu\text{-O}) + 2[\mathrm{CpMo(O)_2}]_2 + 4\mathrm{ZnCl_2(THF)} \tag{3}$$

dark-brown compound $[\mathrm{CpMo(O)}(\mu\text{-O})]_2$ is known[6,18] but is reported as being diamagnetic.[6] We were therefore unable to identify the amorphous black solid as $[\mathrm{CpMo(O)}(\mu\text{-O})]_2$.

Attempts were made to reduce $\mathrm{CpMoCl_2(O)}$ with other reducing agents. There was no apparent reaction with aluminum; addition of $\mathrm{AlCl_3}$ did induce reduction, but only very slowly. Both magnesium and sodium amalgam reduced $\mathrm{CpMoCl_2(O)}$ to red-brown materials, but these could not be adequately characterized.

Structure and Properties of $[\mathrm{CpMoCl(O)}]_2(\mu\text{-O})$. The important structural parameters for $[\mathrm{CpMoCl(O)}]_2(\mu\text{-O})$ are given in Table V, and the structure is shown in Figure 4. It is very similar to that of $[\mathrm{CpMoI(O)}]_2(\mu\text{-O})$ briefly described by Prout and Couldwell[19] and to that of $[\mathrm{Cp^*VI_2}]_2(\mu\text{-O})$.[10] The bridging oxygen atom lies on a crystallographic center of symmetry; therefore, the CpMoX(O) or $\mathrm{Cp^*VI_2}$ units (X = Cl, I) have the trans geometry and the Mo–O–Mo unit is linear. The coordination about each molybdenum is that of a distorted piano stool, as in $\mathrm{CpMoCl_2(O)}$. The high trans influence of the terminal oxygen, which has been observed in other $\mathrm{Cp'ML}_n\mathrm{(O)}$ complexes[10,14,20,21] is apparent here also. The Mo–C(ring) distances vary from 2.41 (1) Å trans to the terminal oxygen (O(2)) to 2.32 (1) Å cis to O(2). The Mo–O(2) distance, 1.668 (7) Å, indicates strong multiple bonding; the distance is even shorter than in $\mathrm{CpMoCl_2(O)}$ (1.740 (6) Å). The Mo–Cl distance, 2.348 (3) Å, is, however, longer than in $\mathrm{CpMoCl_2(O)}$ (2.302 (3) Å). The reason for these differences is that in $[\mathrm{CpMoCl(O)}]_2(\mu\text{-O})$ the molybdenum orbitals available for π-bonding are either involved in the pairing of the single d electron on each molybdenum via the bridging oxygen or in satisfying the bonding requirements of the terminal oxygen. There is no competition by Cl for π-orbitals in $[\mathrm{CpMoCl(O)}]_2(\mu\text{-O})$ as there is in $\mathrm{CpMoCl_2(O)}$.

The $\mathrm{d^1}$–$\mathrm{d^1}$ dimolybdenum complex $[\mathrm{CpMoCl(O)}]_2(\mu\text{-O})$ is diamagnetic, as are $[\mathrm{CpMoI(O)}]_2(\mu\text{-O})$[7] and the centrosymmeric $\mathrm{d^1}$–$\mathrm{d^1}$ divanadium complex $[\mathrm{Cp^*VI_2}]_2(\mu\text{-O})$.[10,22] Other $\mathrm{d^1}$–$\mathrm{d^1}$ dinuclear complexes with oxygen bridges such as $[\mathrm{Mo(S_2P(OEt)_2)_2(O)}]_2(\mu\text{-O})$[23] and $[\mathrm{Mo(S_2COEt)_2(O)}]_2(\mu\text{-O})$[24] are also diamagnetic. As discussed by Cotton and co-workers,[24] the primary requirement for pairing of electrons is that the dπ orbitals on each metal be aligned with a pπ orbital on the bridging oxygen. In the present examples this means that the molecule must have a plane of symmetry containing the M–O–M unit and a plane perpendicular to the M–O–M axis containing the O atom or must have a center of symmetry at the O atom. In the former case linearity of the M–O–M unit is not required, though overlap between the metal dπ orbitals and the oxygen pπ is maximized if the M–O–M unit is linear. The center of symmetry observed in the present cases appears to be due to steric factors that force the Cp′ rings to be trans to one another, since the centrosymmetric structure is also adopted by $\mathrm{d^0}$–$\mathrm{d^0}$ binuclear molecules such as $[\mathrm{Cp^*Mo(O)_2}]_2(\mu\text{-O})$.[25–27] In the $\mathrm{d^0}$–$\mathrm{d^0}$ complex $[\mathrm{Cp^*VCl(O)}]_2(\mu\text{-O})$ the V–O–V angle is not even linear (142°).[28] However $[\mathrm{Cp_2Ti}]_2(\mu\text{-O})$, in which steric factors preclude both a center of symmetry and a plane perpendicular to Ti–O–Ti, has a linear Ti–O–Ti unit but is paramagnetic.[29,30] Thus we conclude that only planes of symmetry are necessary for pairing of the electrons; other symmetry may be imposed by steric factors, which can therefore determine the magnetism.

Experimental Section

General Procedures. The starting material $[\alpha\text{-MoCl_3(O)}]_n$ was purchased from Strem Chemicals Inc.; $(\mathrm{Bu^n})_3\mathrm{Sn(C_5H_5)}$ was prepared by the literature method.[12] **Caution**: Organotin reagents are toxic. All other reagents were reagent grade and were dried and degassed by standard procedures before use. Solvents were predried, stored over $\mathrm{Bu^nLi}$ under vacuum, and distilled under vacuum onto the reagents. All procedures were carried out under argon or vacuum using modified Schlenk-type methods. Infrared spectra were measured (as Nujol mulls between KBr plates) on

---

[18] Couldwell, C.; Prout, K. *Acta Crystallogr.* **1978**, *B34*, 933.

[19] Prout, K.; Couldwell, C. *Acta Crystallogr.* **1980**, *B36*, 1481.

[20] Herrmann, W. A. *J. Organomet. Chem.* **1986**, *300*, 111.

[21] Parkin, G.; Marsh, R. E.; Schaefer, W. P.; Bercaw, J. E. *Inorg. Chem.* **1988**, *27*, 3262.

[22] The magnetic moment of $[\mathrm{Cp^*VI_2}]_2(\mu\text{-O})$ was previously reported as uncertain, due to the presence of paramagnetic impurities.[10] Recent work indicates that the complex is diamagnetic.

[23] Knox, J. R.; Prout, C. K. *Acta Crystallogr.* **1969**, *B25*, 2281.

[24] Blake, A. B.; Cotton, F. A.; Wood, J. S. *J. Am. Chem. Soc.* **1964**, *86*, 3024.

[25] Gomez-Sal, P.; de Jesus, E.; Royo, P.; Vazquez de Miguel, A.; Martinez-Carrera, S.; Garcia-Blanco, S. *J. Organomet. Chem.* **1988**, *353*, 191.

[26] Leoni, P.; Pasquali, M.; Salsini, L.; di Bugno, C.; Braga, D.; Sabatino, P. *J. Chem. Soc., Dalton Trans.* **1989**, 155.

[27] Faller, J. W.; Ma, Y. *J. Organomet. Chem.* **1988**, *340*, 59.

[28] Herberhold, M.; Kremnitz, W.; Kuhnlein, M.; Ziegler, M. L.; Brunn, K. *Z. Naturforsch.* **1987**, *42b*, 1520.

[29] Bottomley, F.; Lin, I. J. B.; Mukaida, M. *J. Am. Chem. Soc.* **1980**, *102*, 5238.

[30] Honold, B.; Thewalt, U.; Herberhold, M.; Alt, H. G.; Kool, L. B.; Rausch, M. D. *J. Organomet. Chem.* **1986**, *314*, 105.

a Perkin-Elmer 683 instrument; NMR spectra were measured on a Varian XL-200 spectrometer and were calibrated against solvent or grease peaks; ESR spectra were run on a locally modified version of a Varian E4 instrument and were calibrated against DPPH. Magnetic moments were measured, in solution, by the Evans method. Microanalyses were by Beller Laboratorium, Göttingen, FRG, and molecular weights (by osmometry) by the Analytische Laboratorium, Engelskirchen, FRG.

Preparation of CpMoCl$_2$(O). To a well-stirred suspension of [MoCl$_3$(O)]$_n$ (4.21 g, 19.3 mmol) in ether (100 cm^3) was added dropwise (Bu^n)$_3$Sn(C$_5$H$_5$) (9.31 g, 26.2 mmol). The resultant mixture was stirred at room temperature for 18 h and then filtered, giving a blue-black solid. This solid was extracted twice with ether (75 cm^3 per extraction), each time for 18 h. The extracts were combined, and the ether removed under vacuum to give a brown oil. This was extracted with toluene (100 cm^3) for 18 h, the extract filtered, and the golden-brown filtrate concentrated to 25 cm^3. Layering with hexane (75 cm^3) gave yellow-brown crystals of CpMoCl$_2$(O), which were removed by filtration, washed with toluene (5 cm^3) and hexane (10 cm^3) and dried under vacuum. Yield 1.99 g, 8.00 mmol, 41%. Anal. Found: C, 24.2; H, 2.0; Cl, 28.4. Calcd for C$_5$H$_5$Cl$_2$MoO: C, 24.2; H, 2.0; Cl, 28.6. Infrared: 946 cm^{-1} (ν(Mo=O)). NMR (^{1}H, ^{2}H$_8$ THF solution): 47.95 ppm, very broad. ESR (toluene solution, 295 K): single broad resonance at $g = 1.96$. The compound was also characterized by X-ray diffraction (see below).

Reduction of CpMoCl$_2$(O) with Zinc Powder: Formation of {[CpMoCl]$_4$(μ-O)$_6$}(ZnCl(THF))$_2$. To a solution of CpMoCl$_2$(O) (0.74 g, 2.99 mmol) in THF (100 cm^3) was added zinc powder (0.21 g, 3.21 mmol). The mixture was stirred. It changed color from yellow-brown to a deep red-brown within 5 min, without evolution of gas or heat. After stirring for 1 h, the mixture was filtered to remove excess zinc. The brick-red filtrate was reduced to 25 cm^3 under vacuum and then layered with ether (25 cm^3). After this was set aside for 5 h, a dark red-brown precipitate of {[CpMoCl]$_4$(μ-O)$_6$}(ZnCl(THF))$_2$ formed. This was collected by filtration, washed with THF (10 cm^3) and ether (10 cm^3), and dried in vacuum. Yield 0.28 g, 0.023 mmol 45%. Anal. Found: C, 26.8, 26.6; H, 2.7, 2.8; Cl, 16.7, 16.9. Calcd for C$_{28}$H$_{36}$Cl$_6$Mo$_4$O$_8$Zn$_2$: C, 27.4; H, 3.0; Cl, 17.3. Infrared: ν_{asym}(Mo–O–Mo) 728 cm^{-1}. ^{1}H NMR (200 MHz ^{2}H$_8$-THF solution): 6.44, 6.38 ppm, singlets of relative intensity 1:1 (C$_5$*H*$_5$). Molecular wt (osmometric, THF solution) 1080; calcd 1228. Mass spectrum (negative ion FAB): *m/e* 1218 (M − H)$^-$, 983–976, Cp$_4$Mo$_4$Cl$_5$O$_6$Zn$^-$, Cp$_3$Mo$_4$Cl$_5$O$_6$Zn(THF)$^-$, Cp$_4$Mo$_4$Cl$_5$O$_6$(THF)$^-$; 837, CpMo$_4$Cl$_5$O$_5$Zn(THF).

Oxidation of {[CpMoCl]$_4$(μ-O)$_6$}(ZnCl(THF))$_2$ by O$_2$: Formation of [CpMoCl(O)]$_2$(μ-O) and [ZnCl(THF)(μ-Cl)]$_\infty$. A solution of {[CpMoCl]$_4$(μ-O)$_6$}(ZnCl(THF))$_2$ (0.50 g) in THF (75 cm^3) was incubated with 1 atm of pure O$_2$, with stirring, for 18 h. The color of the brick-red solution changed to gold-black. After filtration the solution was set aside. Over 8 days it deposited two crystalline products and an amorphous black solid, which were manually separated. One product was colorless and extremely hygroscopic, [ZnCl(THF)(μ-Cl)]$_\infty$. This was characterized by X-ray crystallography.[15] The second product was green [CpMoCl(O)]$_2$(μ-O), also characterized by X-ray crystallography (see below) and by the following data. Infrared: 917 cm^{-1} (ν(Mo=O)); 729 (ν_{asym} Mo–O–Mo). NMR (^{1}H, ^{2}H$_8$-toluene solution): 6.66 ppm, s (C$_5$*H*$_5$). The black amorphous solid showed a single very broad resonance envelope centered at 4 ppm in the ^{1}H NMR spectrum and only broad absorptions attributable to Cp and Mo–O–Mo bridging vibrations at 720 cm^{-1} in the infrared spectrum.

Table VI. Crystal Data, X-ray Diffraction Results, and Refinement Details for CpMoCl$_2$(O) and [CpMoCl(O)]$_2$(μ-O)

	[CpMoCl(O)]$_2$(μ-O)	CpMoCl$_2$(O)
mol formula	C$_{10}$H$_{10}$Cl$_2$Mo$_2$O$_3$	C$_5$H$_5$Cl$_2$MoO
M_r, daltons	440.98	247.85
system	monoclinic	monoclinic
space group	$P2_1/c$	$P2_1/n$
a, Å	6.5136 (5)	6.5963 (8)
b, Å	11.494 (2)	9.7491 (15)
c, Å	9.593 (1)	11.889 (2)
β, deg	107.050 (8)	91.77 (1)
V, Å^3	686.63	764.19
Z	2	4
F(000), electrons	340	476
D_x, Mg m^{-3}	2.13	2.15
T, K	295	295
cryst dimens, mm	0.15 × 0.15 × 0.04	0.36 × 0.20 × 0.08
radtn	Mo Kα	Mo Kα
λ, Å	0.71073	0.71073
μ, cm^{-1}	21.7	23.0
scan mode	$\omega/2\theta$	$\omega/2\theta$
2θ range, deg	2–45	2–50
total no. of reflns	1766	5328
unique reflns	883	1334
obsd reflns	608	1032
obsd criteria	$I > 2.5\sigma(I)$	$I > 2.5\sigma(I)$
no. of refined params	85	51
obsd/param ratio	7.2	20.2
R[a]	0.036	0.063
R_w[b,c]	0.044	0.057
GOF[d]	0.990	1.64
max residual, e Å^{-3}	0.43	2.42
min residual, e Å^{-3}	−0.43	−1.54

[a] $R = (\sum|\Delta F|)/(\sum F_o)$. [b] $R_w = \{(\sum w|\Delta F|^2)/(\sum w(F_o)^2)\}^{1/2}$. [c] $w = 1/(\sigma(F)^2 + 0.001(F)^2)$, σ being obtained from counting statistics. [d] GoF $= \sum w(\Delta F)^2/[$(no. of reflections) − (no. of parameters)$]$.

Table VII. Atomic Parameters and B_{iso} for [CpMoCl(O)]$_2$(μ-O)

	x	y	z	B_{iso},[b] Å^2
Mo	0.98871 (13)[a]	0.43665 (8)	0.17458 (9)	3.33 (4)
Cl	0.7821 (4)	0.2808 (3)	0.0495 (3)	5.57 (16)
O(1)	1	0.5	0	6.0 (6)
O(2)	0.8208 (11)	0.5169 (7)	0.2367 (9)	5.8 (4)
C(1)	1.3379 (20)	0.4887 (14)	0.3043 (16)	6.0 (7)
C(2)	1.3652 (16)	0.3930 (17)	0.2239 (14)	5.8 (8)
C(3)	1.2773 (20)	0.2993 (14)	0.2634 (18)	6.2 (8)
C(4)	1.2398 (23)	0.4474 (20)	0.4027 (13)	7.7 (10)
C(5)	1.1951 (21)	0.3302 (17)	0.3730 (17)	6.5 (8)

[a] Esd's refer to the last digits printed. [b] B_{iso} is the mean of the principal axes of the thermal ellipsoid.

Table VIII. Atomic Positions for the Non-Hydrogen Atoms of CpMoCl$_2$(O)

atom	x	y	z	B_{iso},[c] Å^2
Mo	−0.1781 (1)[b]	0.2732 (1)	0.0285 (1)	3.30
Cl(1)	0.1651 (4)	0.2666 (3)	0.0713 (2)	4.95
Cl(2)	−0.2460 (5)	0.0865 (3)	0.1391 (3)	5.42
O(1)	−0.2633 (11)	0.4098 (7)	0.1085 (6)	4.92
C(1)[a]	−0.0761 (16)	0.2361 (20)	−0.1636 (16)	3.17
C(2)	−0.1840 (16)	0.3617 (20)	−0.1557 (16)	3.17
C(3)	−0.3849 (16)	0.3309 (20)	−0.1243 (16)	3.17
C(4)	−0.4012 (16)	0.1864 (20)	−0.1128 (16)	3.17
C(5)	−0.2104 (16)	0.1278 (20)	−0.1371 (16)	3.17
C(1A)	−0.0941 (19)	0.1959 (18)	−0.1590 (15)	3.52
C(2A)	−0.1244 (19)	0.3401 (18)	−0.1601 (15)	3.52
C(3A)	−0.3298 (19)	0.3659 (18)	−0.1346 (15)	3.52
C(4A)	−0.4264 (19)	0.2377 (18)	−0.1177 (15)	3.52
C(5A)	−0.2807 (19)	0.1326 (18)	−0.1328 (15)	3.52

[a] C(1)–C(5) and C(1A)–C(5A) are the disordered Cp rings. [b] Esd's in parentheses. [c] B_{iso} is the mean of the principal axes of the thermal ellipsoid.

X-ray Crystallography. Dark green crystals of [CpMoCl(O)]$_2$(μ-O) were obtained directly from the reaction between {[CpMoCl]$_4$(μ-O)$_6$}(ZnCl(THF))$_2$ and O$_2$ in toluene. Crystal data are given in Table VI. Brown crystals of CpMoCl$_2$(O) were obtained from THF, from ether, and also from toluene. The crystals were observed in three different monoclinic forms. One had cell dimensions 6.608, 9.764, 11.988 Å, β = 93.1°, space group $P2_1/n$; a second 6.460, 9.731, 6.602 Å, β = 115.4°, space group $P2_1/n$; a third obtained from THF was used for the determination and had the crystal data given in Table VI. Crystals were coated with degassed Apiezon grease and mounted in a sealed tube under argon. Space-group symmetry and intensity data were obtained on an Enraf-Nonius CAD4 diffractometer under the control of the NRCCAD program.[31] Both structures were solved by direct methods; no absorption corrections were made. Details are given in Table VI. Programs used were the NRCVAX suite[32] and SHELX-76.[33] Scattering factors were taken from ref 34.

In $[CpMoCl(O)]_2(\mu\text{-}O)$ the H atoms were allowed to ride on the C atom to which they were attached (r(C–H) = 0.96 Å), and the isotropic thermal parameter of each hydrogen was varied independently. The positional parameters for $[CpMoCl(O)]_2(\mu\text{-}O)$ are given in Table VII and important distances and angles in Table V, and other relevant data have been deposited as supplementary material (see the paragraph at the end of the paper).

The disorder in $CpMoCl_2(O)$ is discussed above. In the final refinement the Mo, Cl, and O atoms were anisotropic. The C_5H_5 ring, which was disordered over two major sites, was refined as two independent rigid bodies, each of half-occupancy, with C–C distances of 1.42 Å and C–H distances of 0.96 Å. Each ring was assigned a single, isotropic, thermal parameter. The final difference Fourier synthesis had "ghost" peaks at approximately 0.85 Å from all atoms, these being due to the slippage discussed above. Positional parameters are listed in Table VIII, important distances and angles in Table I; other data have been deposited as supplementary material.

Acknowledgments. We thank Sarajane MacIntosh for experimental assistance and the donors of the Petroleum Research Fund, administered by the American Chemical Society, the Natural Sciences and Engineering Research Council of Canada, and the Imperial Oil Research Fund for financial support.

Supplementary Material Available: Lists of hydrogen atom positions, U_{ij} values, bond distances and angles, distances to the least-squares planes, and anisotropic thermal parameters for $[CpMoCl(O)]_2(\mu\text{-}O)$ and $CpMoCl_2(O)$ (5 pages); lists of observed and calculated structure factors for $[CpMoCl(O)]_2(\mu\text{-}O)$ and $CpMoCl_2(O)$ (13 pages). Ordering information is given on any current masthead page.

---

(31) Le Page, Y.; White, P. S.; Gabe, E. J. Annual Meeting of the American Crystallographic Association, Hamilton, Ontario, Canada, 1986.

(32) Gabe, E. J.; Lee, F. L.; Le Page, Y. *Crystallographic Computing*; Sheldrick, G. M., Kruger, C., Goddard, R., Eds.; Clarendon Press: Oxford, 1985; Vol. 3, p 167.

(33) Sheldrick, G. M. SHELX-76, University of Cambridge, 1976.

(34) *International Tables for X-ray Crystallography*; Kynoch Press; Birmingham, UK, 1974; Vol. IV.

Organotransition-Metal Metallacarboranes. 15.[1] Regiospecific B-Alkylation of (arene)M($Et_2C_2B_3H_5$) (M = Fe, Ru) and (C_5Me_5)Co($Et_2C_2B_3H_5$) Sandwich Complexes

James H. Davis, Jr., Martin D. Attwood, and Russell N. Grimes*

Department of Chemistry, University of Virginia, Charlottesville, Virginia 22901

Received September 22, 1989

The controlled introduction of hydrocarbon substituents onto specific boron locations in *nido*-metallcarborane complexes of the title classes has been achieved via bridge deprotonation followed by reaction with alkyl or arylalkyl halides. The monodeprotonated complex anions react with MeI, EtBr, p-$MeC_6H_4CH_2Br$, or p-$BrCH_2C_6H_4CH_2Br$ in THF to generate exclusively the B(5)-substituted derivative in each case. This pattern differs strikingly from the corresponding reactions of *nido*-$R_2C_2B_4H_5^-$ carborane anions, which had been shown in an earlier study to give the B(4)- (and equivalent B(6)-) alkylated products with 99% regiospecificity. In the present work, the *B*(*5*)-methyl complexes of Fe, Ru, and Co were each further alkylated via deprotonation/alkyl halide treatments, to give successively the *B*(*4,5*)-dimethyl and *B*(*4,5,6*)-trimethyl derivatives as desired. The alkylated products were isolated in generally high yields; for the three compound classes studied, the *B*-monomethyl complexes are extremely air-stable, but the sensitivity to air increases on further alkylation. Reactions of the $(C_6Me_6)Fe(Et_2C_2B_3H_3)^{2-}$ and $(C_5Me_5)Co(Et_2C_2B_3H_3)^{2-}$ dianions with alkyl iodides result in partial iodination at the B(4) position.

Introduction

In a series of papers we have described methods for the systematic preparation of C- and B-substituted derivatives[2,3] of *nido*-2,3-$C_2B_4H_8$, the conversion of these to arene–transition-metal–carborane double- and triple-decker sandwich complexes,[1,3,4] and the utilization of such complexes as building blocks in constructing stacked or linked-sandwich electron-delocalized systems.[1b,5] One of the long-range objectives of this work is the directed synthesis of electronically active polymers or solid-state networks that are stabilized by cyclic $R_2C_2B_3H_3^{4-}$ or pyramidal $R_2C_2B_4H_4^{2-}$ carborane units and can be tailored to exhibit specific desired properties.[2,3]

Prior to this work our synthetic strategies have centered on assembling sandwich or linked-sandwich systems from *nido*-carborane anions, metals, and arene (or cyclo-

---

[1] (a) Part 12: Davis, J. H., Jr.; Sinn, E.; Grimes, R. N. *J. Am. Chem. Soc.* **1989**, *111*, 4776. (b) Part 13: Davis, J. H., Jr.; Sinn, E.; Grimes, R. N. *Ibid.* **1989**, *111*, 4784. (c) Part 14: Chase, K. J.; Grimes, R. N. *Organometallics* **1989**, *8*, 2492.

[2] (a) Fessler, M. E.; Spencer, J. T.; Lomax, J. F.; Grimes, R. N. *Inorg. Chem.* **1988**, *27*, 3080 and references therein. (b) Boyter, H. A., Jr.; Grimes, R. N. *Inorg. Chem.* **1988**, *27*, 3069, 3075. (c) Davis, J. H., Jr.; Grimes, R. N. *Inorg. Chem.* **1988**, *27*, 4213.

[3] Recent reviews: (a) Grimes, R. N. *Pure Appl. Chem.* **1987**, *59*, 847. (b) Grimes, R. N. In *Advances in Boron and the Boranes*; Liebman, J. F., Greenberg, A., Williams, R. E., Eds.; Molecular Structure and Energetics 5; VCH: New York, 1988; Chapter 11, pp 235–263.

[4] (a) Spencer, J. T.; Grimes, R. N. *Organometallics* **1987**, *6*, 323, 328 and references therein. (b) Attwood, M. A.; Fonda, K. K.; Grimes, R. N.; Brodt, G.; Hu, D.; Zenneck, U.; Siebert, W. *Organometallics* **1989**, *8*, 1300. (c) Grimes, R. N. *Coord. Chem. Rev.* **1979**, *28*, 47.

[5] Merkert, J. M.; Geiger, W. E., Jr.; Davis, J. H., Jr.; Attwood, M. D.; Grimes, R. N. *Organometallics* **1989**, *8*, 1580.

0276-7333/90/2309-1171$02.50/0 © 1990 American Chemical Society